Effect of Staphylococcal δ-Lysin on the Thermotropic Phase Behavior and Vesicle Morphology of Dimyristoylphosphatidylcholine Lipid Bilayer Model Membranes. Differential Scanning Calorimetric, ^{31}P Nuclear Magnetic Resonance and Fourier Transform Infrared Spectroscopic, and X-ray Diffraction Studies†

Karl Lohner,*,‡ Erich Staudegger,‡ Elmar J. Prenner,§ Ruthven N. A. H. Lewis,§ Manfred Kriechbaum,‡ Gabor Degovics,‡ and Ronald N. McElhaney§

Institut für Biophysik und Röntgenstrukturforschung, Österreichische Akademie der Wissenschaften, Steyrergasse 17/VI, A-8010 Graz, Austria, and Department of Biochemistry, University of Alberta, Edmonton, Alberta, Canada T6G 2H7

Received June 9, 1999; Revised Manuscript Received September 21, 1999

ABSTRACT: We investigated the effects of various concentrations of staphylococcal δ-lysin on the thermotropic phase behavior of large multilamellar dimyristoylphosphatidylcholine (DMPC) vesicles by differential scanning calorimetry (DSC), ^{31}P nuclear magnetic resonance (NMR) and Fourier transform infrared (FTIR) spectroscopy, and X-ray diffraction. The DSC studies revealed that at all concentrations, the addition of δ-lysin progressively decreases the enthalpy of the pretransition of DMPC bilayers without significantly affecting its temperature or cooperativity. Similarly, the addition of smaller quantities of peptide has little effect on the temperature of the main phase transition of DMPC bilayers but does reduce the cooperativity and enthalpy of this transition somewhat. However, at higher peptide concentrations, a second phase transition with a slightly increased temperature and a markedly reduced cooperativity and enthalpy is also induced, and this latter phase transition resolves itself into two components at the highest peptide concentrations that are tested. Moreover, our ^{31}P NMR spectroscopic studies reveal that at relatively low δ-lysin concentrations, essentially all of the phospholipid molecules produce spectra characteristic of the lamellar phase, whereas at the higher peptide concentrations, an increasing proportion exhibit an isotropic signal. Also, at the highest δ-lysin concentrations that are studied, the isotropic component of the ^{31}P NMR spectrum also resolves itself into two components. At the highest peptide concentration that was tested, we are also able to effect a macroscopic separation of our sample into two fractions by centrifugation, a pellet containing relatively smaller amounts of δ-lysin and a supernatant containing larger amounts of peptide relative to the amount of lipid present. We are also able to show that the more cooperative phase transition detected calorimetrically, and the lamellar phase ^{31}P NMR signal, arise from the pelleted material, while the less cooperative phase transition and the isotropic ^{31}P NMR signal arise from the supernatant. In addition, we demonstrate by X-ray diffraction that the pelleted material corresponds to δ-lysin-containing large multilamellar vesicles and the supernatant to a mixture of δ-lysin-containing small unilamellar vesicles and discoidal particles. We also show by FTIR spectroscopy that δ-lysin exists predominantly in the α-helical conformation in aqueous solution or when interacting with DMPC, and that a large fraction of the peptide bonds undergo H−D exchange in D_2O. However, upon interaction with DMPC, the fraction of exchangeable amide protons decreases. We also demonstrate by this technique that both of the phase transitions detected by DSC correspond to phospholipid hydrocarbon chain-melting phase transitions. Finally, we show by several techniques that the absolute concentrations of δ-lysin and the thermal history, as well as the lipid:peptide ratio, can affect the thermotropic phase behavior and morphology of peptide−lipid aggregates.

δ-Lysin (also formerly called δ-hemolysin or δ-toxin) is one of a number of cytolytic and cytotoxic polypeptides secreted by most strains of *Staphylococcus aureus* (for reviews, see refs *1*−*3*). This 26-residue, surface-active polypeptide lyses erythrocytes and many other types of mammalian cells, as well as intracellular organelles and bacterial protoplasts (*1*−*3*). It also activates the membrane

† This work was supported by the Fonds zur Forderung der Wissenschaftlichen Forschung in Österreich (P10932-Gen to K.L.) as well as by Operating and Major Equipment grants from the Medical Research Council of Canada, and by Major Equipment grants from the Alberta Heritage Foundation for Medical Research (R.N.M.). E.J.P. was supported by a Fellowship from the Alberta Heritage Foundation for Medical Research. We are indebted to Dr. Brian D. Sykes for the availability of time on the NMR spectrometer and for his assistance in the interpretation of data.

* To whom correspondence should be addressed: Institut für Biophysik und Röntgenstrukturforschung, Österreichische Akademie der Wissenschaften, Steyrergasse 17/VI, A-8010 Graz, Austria. Telephone: 43-316-812004-18. Fax: 43-316-812367. E-mail: fibrkarl@mbox.tu-graz.ac.at.

‡ Österreichische Akademie der Wissenschaften.

§ University of Alberta.

10.1021/bi9913101 CCC: $18.00
Published on Web 11/20/1999

phospholipase A_2 of mouse fibroblasts, releasing arachidonic acid and stimulating prostaglandin synthesis in these cells (*2*). Upon injection, δ-lysin is lethal for many laboratory animals, at least at relatively high doses, and increases vascular permeability in rabbits (*4*). However, since the action of this polypeptide is not cell specific and is inhibited by serum and phospholipid dispersions (*1*, *5*), its primary mode of action appears to be on the membrane lipid bilayer of its target cells, although it may also have secondary effects in certain cells or tissues (*1*−*3*).

The amino acid sequence of the best-studied form of δ-lysin has been determined to be *N*-formyl-MAQDIIS-TIGDLVKWIIDTVNKFTKK (*6*). Although this peptide has no net charge at neutral pH, it contains four positive and four negative charges, the positive charges arising from the four lysine residues, including the carboxy terminal dilysine sequence, and the negative charges arising from the three aspartate residues and the carboxy terminus. Also, δ-lysin contains 14 hydrophobic and 4 polar but nonionizable amino residues. Moreover, the charged and hydrophobic or non-ionizable amino acid residues have a regular periodic distribution along the polypeptide chain. δ-Lysin has been shown by CD, NMR, and FTIR[1] spectroscopy to exist predominantly in an α-helical form in various organic solvents or solvent/water mixtures (*7*−*9*) or when bound to lipid micelles (*10*) or lipid bilayers (*11*−*13*). However, in water, this polypeptide has variously been reported to be unstructured (*10*) or to contain moderate (*7*) or high (*14*) amounts of α-helical structure, which is probably dependent on its concentration and state of aggregation (*13*). In its biologically relevant lipid-bound form, δ-lysin probably exists as an amphiphilic α-helix with the clustering of charged and nonpolar amino acid residues on different sides of the helix (*15*, *16*). Such an amphipathic, rod-like structure would account for the ability of this polypeptide to form aggregates in water, to form stable monolayers at the air−water interface (*7*), and to bind to phospholipids and blood lipoproteins (*1*), as well as for its appreciable solubility in both water and organic solvents (*7*, *8*). It has been proposed that the amphiphilic, α-helical δ-lysin molecules probably lie parallel to the surface of the target membrane, with the hydrophobic side chains of the nonpolar amino acid penetrating into the hydrophobic core of the lipid bilayer while the charged amino acid residues bind to the lipid polar headgroups near the membrane surface (*13*, *15*, *16*). Indeed, tryptophan fluorescence experiments with δ-lysin and synthetic analogues suggest exactly this arrangement when associated with lipid micelles and bilayers (*12*, *13*). However, an FTIR spectroscopic determination of the orientation of δ-lysin when bound to lipid bilayer membranes suggested a random orientation of the polypeptide molecule with respect to the bilayer plane (*11*).

The aggregation state of δ-lysin has been shown to depend on the polarity and pH of the aqueous solvent in which it is dispersed as well as on the concentration of the peptide that is present. In water at neutral pH, this polypeptide has been reported to exist primarily as a monomer at very low concentrations, but to form much larger aggregates as the polypeptide concentration increases (*8*, *13*, *17*, *18*). Moreover, the α-helical content of δ-lysin in water appears to increase with the concentration and degree of aggregation of the polypeptide (*13*). However, at extremes of pH or in the presence of chaotropic agents, partial disaggregation into dimeric of tetrameric species may occur (*8*, *17*). The state of aggregation of δ-lysin when bound to natural or model lipid bilayer membranes is currently an important but unresolved question.

In addition to lysing erythrocytes and many other cell types (*1*−*3*), at sufficiently high peptide concentrations δ-lysin also lyses phospholipid bilayer vesicles (*19*) and induces vesicle fusion (*20*). At lower peptide concentrations, δ-lysin can penetrate phospholipid monolayers (*21*) and induce permeability increases in phospholipid bilayers (*19*, *22*). Although most studies of δ-lysin−phospholipid interactions have used exclusively PC model membranes, Bhakoo et al. (*21*, *22*) have utilized lipid monolayers and bilayers generated from a number of different phospholipids. Interestingly, the penetration of this peptide into lipid monolayers was reported to be essentially independent of the structure of the phospholipid polar headgroup or of the length or degree of unsaturation of the hydrocarbon chains (*21*). However, the ability of this peptide to permeabilize lipid bilayers was reported to be significantly greater for negatively charged phospholipids than for zwitterionic phospholipids and greater for shorter-chain, unsaturated phospholipids than for longer-chain, saturated phospholipids (*22*).

The effect of δ-lysin on the thermotropic phase behavior, and on the organization and dynamics, of PC model membranes has been studied using several physical techniques. Lohner et al. (*23*) studied the effect of δ-lysin on the thermotropic phase transitions of DPPC vesicles using DSC and TSD. Both techniques reported that the pretransition of this lipid was progressively reduced and eventually abolished completely at an *R* value of about 30:1. The DSC results indicated no change in the temperature and only a small decrease in the enthalpy of the main phase transition over this concentration range of the peptide, although the presence of a broad endothermic component at higher temperatures was detected at the highest polypeptide concentration that was tested. The TSD studies also revealed that the volume change at the main phase transition was progressively reduced by the presence of δ-lysin. Dufourcq et al. (*24*), using solid state ^{2}H NMR and ^{31}P NMR spectroscopy of hydrocarbon chain perdeuterated DPPC vesicles, reported that δ-lysin, even at relatively high concentrations (lipid:polypeptide molar ratio of 10:1), did not alter the overall bilayer structure or the orientational order of the hydrocarbon chains below the lipid phase transition temperature, although it did significantly disorder the polar

[1] Abbreviations: DSC, differential scanning calorimetry; TSD, temperature scanning densitometry; ^{31}P NMR, ^{31}P nuclear magnetic resonance; MLV, multilamellar vesicle; PC, phosphatidylcholine; FTIR, Fourier transform infrared; C═O, carbonyl; CH_2, methylene; DMPC, dimyristoylphosphatidylcholine; DPPC, dipalmitoylphosphatidylcholine; POPC, 1-palmitoyl-2-oleoylphosphatidylcholine; T_p, phase transition temperature for the transition from the lamellar gel ($L_{\beta'}$) to the lamellar ripple ($P_{\beta'}$) phase; T_m, phase transition temperature for the transition from the lamellar ripple ($P_{\beta'}$) to the lamellar liquid-crystalline (L_α) phase; L_c', lamellar crystalline phase with tilted hydrocarbon chains; ΔH, transition enthalpy; $\Delta T_{1/2}$, width of the DSC endotherm at half-height; *R*, phospholipid:peptide molar ratio; d_{disk}, diameter of the lipid disk; $d_{particle}$, diameter of the lipid particle; d_m, thickness of the lipid bilayer; D_{max}, maximum particle dimension; $p(r)$, pair distance distribution function; $p_t(r)$, pair distance distribution function of bilayer thickness; SAXS and WAXS, small- and wide-angle X-ray scattering, respectively.

headgroups. However, above the phase transition temperature, δ-lysin was reported to order the DPPC hydrocarbon chains at lower temperatures (45 °C) but to disorder them at higher temperatures (65 °C) in the liquid-crystalline state, and to have a smaller disordering effect on the lipid polar headgroups. Moreover, at very high δ-lysin concentrations (R = 4:1), isotropic ^{31}P NMR spectra were observed, indicating the formation of small, rapidly tumbling peptide−lipid particles. These workers also reported that at lower concentrations, δ-lysin did not alter the gel to liquid-crystalline phase transition temperature of DPPC vesicles but that very high concentrations of peptide decrease this temperature. Similar results using the same techniques, but with specifically deuterated polar headgroups on POPC, were later reported by Rydal and Macdonald (*25*), who also showed that δ-lysin generally disordered the phosphorylcholine headgroup in the liquid-crystalline phase but did not produce any change in the tilt of the polar headgroup due to a change in the net bilayer surface charge. These latter workers also reported that at R values between 10:1 and 5:1, two lipid populations were present, one consisting of slowly tumbling bilayer vesicles and the other of rapidly tumbling, apparently nonlamellar structures, but that only the latter population was present at R values of ≤5:1.

Differential scanning calorimetry is a powerful thermodynamic technique for probing the nature and stoichiometry of lipid−polypeptide and lipid−protein interactions, and for providing information about the location and state of aggregation of polypeptides and proteins in their lipid-bound state (for a review, see ref *26*). In the study presented here, we utilized DSC for the first time to study the effects of high as well as low concentrations of δ-lysin on the thermotropic phase behavior of a phospholipid model membrane. We also employed ^{31}P NMR spectroscopy to study the effects of this polypeptide on the size and nature of the lipid−polypeptide complexes formed in our experiments, paying particular attention to determining the dependence of the onset of the formation of small, freely tumbling lipid−polypeptide particles on δ-lysin concentration. Also, FTIR spectroscopy was used to evaluate the conformational disposition of the peptide in solution and in association with lipid and to evaluate the effects of this peptide on the structure and organization of its lipid bilayer host. An X-ray diffraction analysis of the structure of these small δ-lysin−DMPC particles was also carried out. We selected large MLVs of DMPC as our lipid bilayer model membrane for these studies, because their gel to liquid-crystalline phase transition is very cooperative and occurs at a convenient temperature (23 °C) (*27*), and because δ-lysin has been reported to have a particularly large effect on the permeability of shorter-chain PC vesicles (*22*).

MATERIALS AND METHODS

Materials. Dimyristoylphosphatidylcholine (DMPC) was obtained from Avanti Polar Lipids (Alabaster, AL) and used without further purification. Staphylococcal δ-lysin was prepared from *S. aureus* strain NTCT 10345 and purified as described by Kreger et al. (*4*), followed by precipitation from an aqueous solution with 1 M trichloroacetic acid and dialysis against distilled water. The purity was assessed by ultraviolet and infrared spectroscopy and was at least as good as that reported by Kreger et al. (*4*).

Preparation of Lipid−Peptide Samples. A sample of pure lyophilized DMPC was dissolved in chloroform (redistilled before use) and spread as a thin film on the walls of a clean glass tube by the slow removal of the solvent. After removal of any residual traces of solvent in vacuo overnight, a known volume of a standardized aqueous solution of δ-lysin was added to obtain the desired lipid:peptide ratio. The mixture was then warmed to 45 °C (fluid phase of DMPC), vortexed vigorously for 3−4 min, and then incubated at 45 °C for 1 h prior to the measurements. The DMPC concentrations were 1−4, 10−15, 25−35, and 100 mg/mL for the DSC, ^{31}P NMR spectroscopic, FTIR spectroscopic, and X-ray diffraction studies, respectively.

Differential Scanning Calorimetry. Calorimetric measurements were taken in a Microcal MC-2 high-sensitivity differential scanning calorimeter at a heating rate of 12 °C/h. In a typical experiment, a freshly prepared sample (1.23 mL) was equilibrated at 17 °C (a temperature between the T_p and T_m of DMPC) and a heating thermogram was recorded. The same sample was then quickly equilibrated at 0−4 °C before a second heating thermogram was recorded, and finally, it was equilibrated at 0−4 °C overnight before a third heating thermogram was recorded. The lipid concentration of each sample was determined by gas−liquid chromatography using methods previously described (*28*). The temperature and enthalpy values reported in Tables 1 and 2 are the averages of three heating scans each performed on two independently prepared samples, for a total of six determinations for each R value that was examined.

^{31}P NMR Spectroscopy. Proton-decoupled ^{31}P NMR spectra were recorded on a Nicolet NT-300WB spectrometer operating in the Fourier transform mode with quadrature detection. The spectra were acquired with a spectral width of ±31.25 kHz. Other details pertinent to data acquisition and processing were as described by Mantsch et al. (*29*).

FTIR Spectroscopy. Infrared spectra of dried samples of staphylococcal δ-lysin were obtained by applying diffuse reflectance methods to lyophilized powders of the peptide with the aid of a Spectra-Tech diffuse reflectance accessory. Solution spectra of the peptide were obtained with samples dissolved in a D_2O-based phosphate buffer composed of 50 mM phosphate, 50 mM NaCl, and 1 mM NaN_3 (pH 7.4). Approximately 1 mg of the peptide was dissolved in 50 μL of the buffer, and the solution was squeezed between the CaF_2 windows of a heatable liquid cell (equipped with a Teflon spacer) to form a 25 μm film. Once the sample had been mounted in the sample holder of the instrument, the sample temperature could be controlled (between −20 and 90 °C) by an external, computer-controlled circulating water bath.

The preparation of lipid and lipid−δ-lysin samples for FTIR spectroscopy was accomplished by two methods. For routine measurements, the sample preparation methodology was comparable to that used for the DSC and NMR spectroscopic measurements. Specifically, 1−2 mg samples of the lipid were dissolved in chloroform and spread as a thin film on the sides of a clean glass tube. After removal of the solvent in vacuo, the film was hydrated with 75−100 μL of a solution of the peptide in the D_2O-based phosphate buffer described above to obtain the required lipid:peptide ratio, and the dispersion so formed was squeezed between the CaF_2 windows of a heatable liquid cell as described

Table 1: Characterization of the Thermotropic Phase Behavior of Mixtures of δ-Lysin and Dimyristoylphosphatidylcholine

(A) The Pretransition

lipid:peptide molar ratio	T_p (°C)	$\Delta T_{1/2}$ (°C)	ΔH (kcal/mol)
1:0	12.8 ± 0.3	2.3 ± 0.5	0.9 ± 0.1
500:1	12.8	2.2	0.6
250:1	12.1	2.0	0.4
125:1	11.8	2.4	0.3
62.5:1	12.9	2.2	0.2
30:1	ND[a]	ND[a]	ND[a]
15:1	ND[a]	ND[a]	ND[a]

(B) The Gel to Liquid-Crystalline Phase Transition

lipid:peptide molar ratio	sharp component			broad component			total enthalpy (kcal/mol)
	T_m (°C)	$\Delta T_{1/2}$ (°C)	ΔH (kcal/mol)	T_m (°C)	$\Delta T_{1/2}$ (°C)	ΔH (kcal/mol)	
1:0	23.7 ± 0.1	0.25 ± 0.03	0.9 ± 0.2	−	−	−	5.9 ± 0.3
500:1	23.7	0.36	4.4	−	−	−	4.4
250:1	23.6	0.46	3.7	−	−	−	3.7
125:1	23.7	0.47	3.5	−	−	−	3.5
62.5:1	23.7	0.48	2.8	25.1 ± 0.3	4.0 ± 0.2	0.6 ± 0.1	3.4
30:1	24.0	0.46	2.0	25.1	3.9	0.9	2.9
15:1	23.8	0.55	0.4	27.2[b]	≅5.0	1.1	1.5

[a] ND, not determined (although a definite pretransition endotherm could be detected at high instrumental sensitivity settings, the quality of the thermograms did not justify the determination of exact temperature and enthalpy values). [b] Appears to be composed of two components centered near 26.4 and 29.2 °C.

Table 2: Effect of Absolute Peptide Concentration on the Thermodynamic Properties of the Gel to Liquid-Crystalline Phase Transition in 62.5:1 Molar Ratio Mixtures of DMPC and δ-Lysin

peptide concentration (μg/mL)	gel to liquid-crystalline phase transition	
	T_m (°C)	ΔH (kcal/mol)
69	23.7 ± 0.1	3.7 ± 0.2
138	23.7	3.4
173	23.6	2.5
207	23.6	2.5
276	23.8	2.5

above. For experiments designed to monitor and assess the rate and extent of H−D exchange, samples were prepared by first codissolving the lipid and peptide in methanol. The lipid/δ-lysin mixture was then spread as a thin film on the sides of a clean glass tube, and after removal of the last traces of the solvent in vacuo, the sample was hydrated with 75−100 μL of the D_2O-based phosphate buffer described above, and mounted on the heatable liquid cell. The samples produced with this procedure exhibited behavior similar to those prepared by the other methodologies described herein. Its use in the H−D exchange experiments was preferred over the other method because it enabled faster sample preparation under conditions where we could exercise greater control of the temperature during sample preparation. With all samples, FTIR spectra were recorded with a Digilab FTS-40 infrared spectrometer (Digilab, Cambridge, MA) using data acquisition parameters comparable to those described by Mantsch et al. (*29*). The data were processed using computer programs obtained from Digilab Inc. and the National Research Council of Canada, and were plotted using the Origin software program (Microcal Software Inc., Northampton, MA).

X-ray Diffraction. Small- and wide-angle X-ray diffraction experiments were performed on a modified Kratky compact camera (HECUS-MBraun-Graz, Graz, Austria), which allows simultaneous recording of diffraction data in both the small- and wide-angle regions as described previously (*30*). Ni-filtered CuKα radiation ($\lambda = 0.154$ nm) originating from a rotating Rigaku-Denki X-ray generator with a Cu anode operating at 50 kV and 80 mA was used. The camera was equipped with a Peltier-controlled variable-temperature cuvette (temperature precision of ±0.1 °C) and a linear one-dimensional position-sensitive OED 50-M detector (MBraun, Garching, Germany). Calibration in the small-angle region was performed with silver stearate and in the wide-angle region with *p*-bromobenzoic acid standards. Temperature control and data acquisition were achieved by programmable temperature control equipment (MTC-2.0, HECUS-MBraun-Graz). Samples were measured in quartz capillaries with a 1 mm diameter and a 100 μm wall thickness, which were assembled in a steel cuvette holder allowing good thermal contact to the thermostating unit and reproducible alignment in the X-ray beam. The samples were equilibrated at their respective temperatures for 15 min before opening the shutter and starting the X-ray measurements. Multiplexed exposure times of 1000 s each were chosen for both the small- and wide-angle regions for pure DMPC samples. Longer exposure times were used for the lipid/peptide samples to yield appropriate signal-to-noise levels to allow analysis in terms of the indirect Fourier transformation method (*31*). Scattering curves, i.e., scattered X-ray intensities as a function of the scattering angle 2Θ, converted into reciprocal units with the equation $h = 4(\pi/\lambda)\sin(\Theta)$ or $s = h/(2p)$, with λ being the wavelength of the X-rays and 2Θ the scattering angle with respect to the incident X-ray beam, were measured.

Briefly, the numerical values of the pair distance distribution functions $p(r)$ and $p_t(r)$ of the lamellae in the axial direction were computed after background subtraction and normalization of the respective buffer blank curve and data point reduction of the difference curve by a funneling routine. The data were corrected for instrumental broadening by using the program ITP of Glatter (*32*) and resulted in desmeared data, which were interpreted in real space in terms of their pair distance distribution function (*32*−*34*). The pair distance distribution function represents a histogram of distances

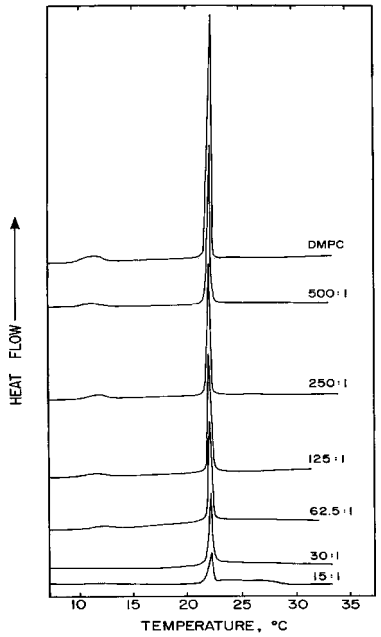

FIGURE 1: High-sensitivity DSC heating endotherms of DMPC/δ-lysin mixtures at lipid:peptide molar ratios of 1:0, 500:1, 250:1, 125:1, 62.5:1, 30:1, and 15:1. The thermograms were all recorded at 11.64 °C h^{-1} after equilibration of the samples at 0−4 °C.

inside the particle weighted with the electron densities at their end points, and it vanishes beyond the distance D_{max}, which represents its maximum particle dimension.

Simulations of selected scattering curves, i.e., calculation of the theoretical scattering curves, and their $p(r)$ functions from cylindrically shaped models (disks with centrosymmetrical inhomogeneity in the axial and radial directions) were carried out by using analytical formulas and numerical integration procedures (*35*), and were subjected to subsequent Fourier transformations by the program ITP as in the case with the experimental scattering curves.

RESULTS

Differential Scanning Calorimetric Studies. A series of high-sensitivity DSC heating thermograms of large multilamellar vesicles composed of DMPC alone, and of DMPC/δ-lysin mixtures, are presented in Figure 1. In all of these samples, the DMPC concentration was held constant at 1 mg/mL, increasing quantities of δ-lysin were added to vary the R value from 500:1 to 15:1, and the samples were equilibrated overnight at low temperatures (0−4 °C) before heating. We found that the DSC thermograms obtained were somewhat dependent on the thermal history of the sample, in that the phase transitions observed in the heating scans of samples not incubated overnight at low temperatures exhibited a decreased cooperativity, particularly at lower peptide concentrations. However, the midpoint temperatures and enthalpies of the phase transitions observed by DSC did not change significantly under these conditions. We therefore present only the data from samples annealed at low temperatures here.

The DSC heating thermogram of DMPC alone exhibits two thermal events, a lower-temperature, less energetic endotherm centered near 14 °C and a higher-temperature, more energetic endotherm centered near 24 °C, as expected. These thermal events correspond to the well-characterized pretransition (i.e., the $L_{\beta'}-P_{\beta'}$ phase transition) and the main or chain-melting (i.e., the $P_{\beta'}-L_{\alpha}$) phase transition of DMPC, respectively. Under these experimental conditions, the subtransition (i.e., the $L_{c'}-L_{\beta'}$ phase transition) is absent, as sufficient time for the formation of significant amounts of the $L_{c'}$ phase has not elapsed. For a more detailed description of the thermotropic phase behavior of DMPC and the other members of the homologous series of *n*-saturated diacyl PCs, refer to Lewis et al. (*27*) and to the references therein.

The incorporation of increasing quantities of δ-lysin has an effect on both the pretransition and main transition of DMPC bilayers. As illustrated in Figure 1 and Table 1, the pretransition temperature and cooperativity are not significantly affected by the presence of peptide, even when relatively high amounts of δ-lysin are present. However, the enthalpy of the pretransition decreases progressively with increases in the peptide concentration and falls to low values at the higher peptide concentrations, making the pretransition difficult to detect by DSC. Please note, however, that the pretransition is not abolished completely even at very high δ-lysin concentrations, as DSC runs at instrumental sensitivities higher than those utilized in Figure 1 clearly show a pretransition endotherm.

The effect of the addition of increasing quantities of δ-lysin on the gel to liquid-crystalline or main phase transition of at least initially multilamellar vesicles of DMPC is also illustrated in Figure 1. Note that at lower peptide concentrations ($R \geq 125:1$), only a single fairly cooperative endotherm is present in the DSC heating thermograms. However, at higher peptide concentrations ($R \leq 62.5:1$), a second broader component of the DSC endotherm also appears and becomes more prominent relative to the sharp component. At the highest peptide concentration that was examined ($R = 15:1$), the broad component in turn resolves itself into two overlapping subcomponents. The molecular basis of these effects of δ-lysin on the thermotropic phase behavior of DMPC/δ-lysin mixtures will be discussed below.

The thermodynamic parameters of the sharp and broad components of the DSC endotherms of DMPC/δ-lysin mixtures as a function of peptide concentration are also provided in Table 1. The temperature of the sharp component changes little if at all with increases in δ-lysin concentration, and the width of this component, as measured by the $\Delta T_{1/2}$ value, increases only modestly. However, the transition enthalpy of the sharp component decreases markedly upon the addition of low concentrations of peptide but decreases progressively less markedly with further increases in peptide concentration (Figure 2). In contrast, the broad component, which appears only at higher peptide concentrations, is initially centered at a higher temperature (about 25 °C) than the sharp component, but resolves itself into two separate components centered near 24 and 27 °C at the highest peptide concentration that was tested. The cooperativity of the broad component (or subcomponents), again expressed as $\Delta T_{1/2}$ values, is also markedly lower than that of the sharp component. Also, as illustrated in Figure 2, the enthalpy of the broad component of the DSC endotherm initially increases, and reaches a maximum at higher peptide concentrations. The net result is that the total enthalpy associated with the overall lipid chain-melting phase transition of this system at first decreases rapidly at lower peptide concentrations, approaches a plateau at intermediate concentrations,

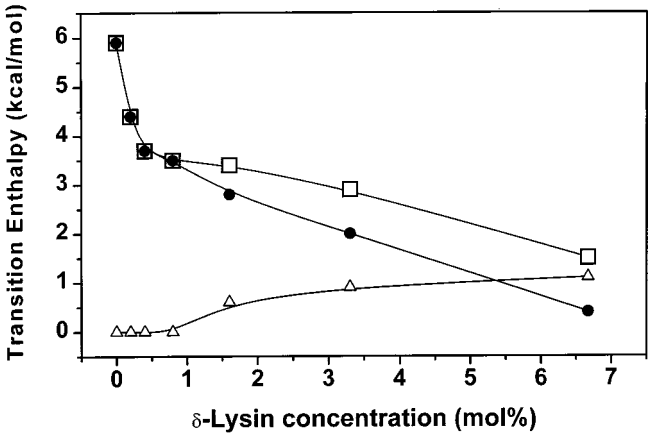

FIGURE 2: Plots of the total enthalpy (□) of the DMPC chain-melting phase transition, and of the sharp (●) and broad (△) components thereof, as a function of δ-lysin concentration.

and then again decreases at a progressively faster rate at the highest peptide concentrations that were tested. A molecular explanation for these variations in the temperature, cooperativity, and enthalpy of the DMPC bilayer chain-melting phase transition with increasing δ-lysin concentrations will be offered below.

The appearance of multiple components in the gel to liquid-crystalline phase transition of DMPC/δ-lysin mixtures at high peptide concentrations suggested the possibility that two (or possibly three) distinct populations of lipid−peptide aggregates might exist under these conditions. To explore this possibility, DMPC/δ-lysin mixtures having an *R* value of 15:1 were subjected to centrifugation to determine if multiple populations of lipid−peptide aggregates could be resolved. Centrifugation of this sample resulted in the formation of a white pellet and an opaque supernatant. Both the pellet and the supernatant contained DMPC and δ-lysin, but the DMPC:peptide molar ratio of the supernatant (approximately 10−15:1) was higher than that of the pellet (about 50−100:1). An examination of the pellet and the supernatant by X-ray diffraction techniques revealed that the former consists primarily of δ-lysin-containing large MLVs while the latter consists of a mixture of δ-lysin-containing small unilamellar DMPC vesicles and small DMPC/δ-lysin discoidal particles, the nature of which is discussed below.

The resuspended peptide-containing large multilamellar vesicles and the smaller lipid−protein aggregates were analyzed separately by DSC to determine whether the thermotropic phase behavior of these two fractions differed. In fact, the DSC thermograms obtained from these two samples do differ markedly as illustrated in Figure 3. The DSC trace of the δ-lysin-containing large multilamellar vesicles exhibits the pretransition and main transition endothermic components observed in the original sample, but lacks the broad component present at higher temperatures (see Figure 3B). Similarly, the DSC thermogram of the smaller lipid−peptide aggregates does not exhibit the pretransition and main transition endotherms but exhibits only the broad, two-component, higher-temperature endotherm observed in the original sample (see Figure 3C). Moreover, if these two fractions are combined in their original proportions, a DSC thermogram closely resembling that of the original preparation is obtained (see Figure 3A). These results indicate that the complex thermotropic phase behavior

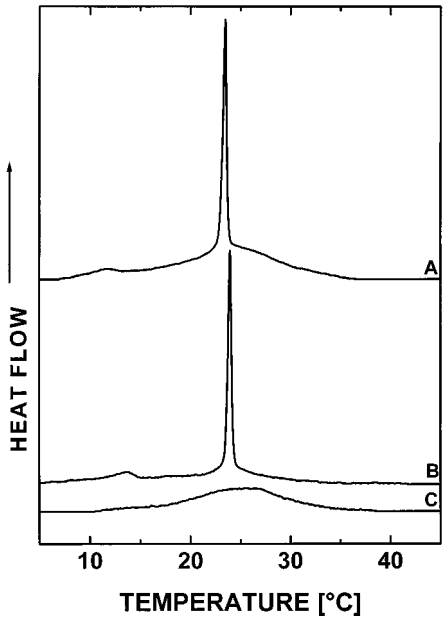

FIGURE 3: High-sensitivity DSC thermograms of mixtures of DMPC/δ-lysin (molar ratio of 15:1) which have been separated into supernatant (B) and pellet fractions (C) by centrifugation for 15 min at 15 000 rpm. A thermogram for the recombined supernatant and pellet fractions is also shown (A).

observed only at relatively high δ-lysin concentrations ($R \leq 62.5$:1) is due to the presence of three different types of lipid−peptide aggregates in the sample. Note also that at an *R* value of 15:1, only about 10% of the DMPC remains as large MLVs in the pellet and yet the transition enthalpy of this fraction represents almost half of the total enthalpy (see Figure 2). This latter result indicates that the intrinsic thermotropic phase behavior of aqueous suspensions of DMPC is considerably more perturbed by the presence of δ-lysin in the small lipid−peptide aggregates induced by the presence of higher concentrations of peptide than it is in the large MLVs present at all peptide concentrations. The possible structural basis for this difference in the effect of δ-lysin on DMPC thermotropic phase behavior will be discussed later.

A number of workers have reported that in aqueous solution, δ-lysin tends to form multimeric aggregates, the size of which may be dependent upon the concentration of the peptide (*8*, *13*, *17*, *18*). To evaluate the effect of absolute peptide concentration on the interaction between δ-lysin and DMPC, we prepared mixtures in which the molar ratio of lipid to added peptide was held constant (62.5:1) but with different absolute concentrations of δ-lysin (range of 70−280 μg/mL) and DMPC. Despite the increase in absolute peptide and lipid concentrations, the DSC thermograms all exhibit heating endotherms exhibiting both the pretransition and gel to liquid-crystalline phase transition events, as well as the broad component characteristic of the heating endotherms at this lipid:peptide ratio (data not presented). However, it is clear that the increase in the absolute peptide concentration, although not resulting in a significant change in the phase transition temperature, is accompanied by changes in the widths of the gel to liquid-crystalline phase transition, as well as in the relative contributions of the broad and sharp components to the total enthalpy of the events occurring near 24 °C. In particular, the cooperativity of the sharp component of the DSC endotherm decreases and the

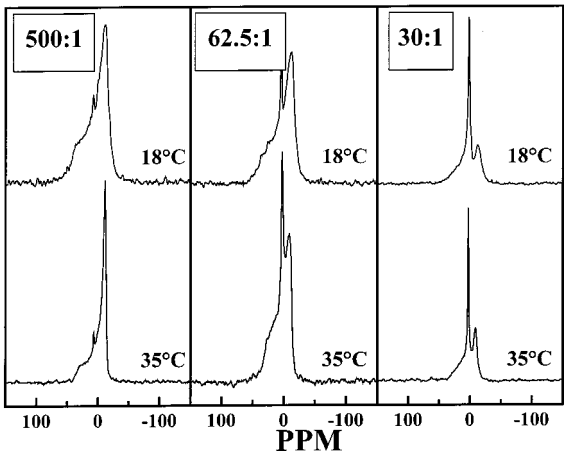

FIGURE 4: Proton-decoupled ^{31}P NMR spectra of mixtures of δ-lysin and DMPC taken at temperatures below and above the main phase transition temperature of DMPC. The mixtures of δ-lysin and DMPC were at molar ratios of 500:1, 62.5:1, and 30:1.

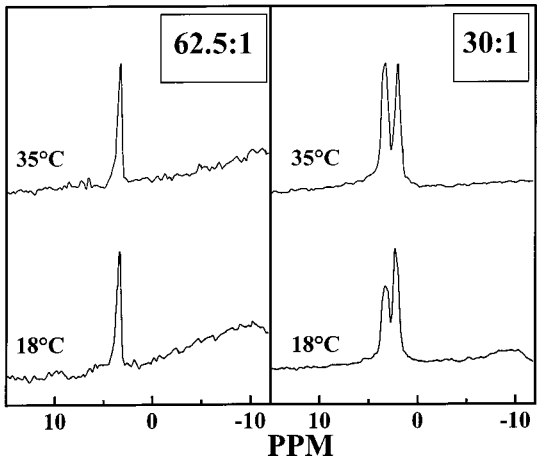

FIGURE 5: Proton-decoupled ^{31}P NMR spectra of a mixture of δ-lysin and DMPC at molar ratios of 62.5:1 and 30:1. The spectra were taken at temperatures below and above the main phase transition temperature of the bulk lipid phase, and are resolution-enhanced and plotted on an expanded scale to better show the fast-tumbling component of the NMR spectrum.

calculated total enthalpy changes (Table 2) are significantly lower at the higher peptide concentrations. Furthermore, the broad component also contributes a larger fraction to the total enthalpy change at the higher peptide concentrations (Table 2). However, this effect does not vary continuously with the absolute peptide concentration but appears to saturate at higher concentrations. Moreover, the magnitude of these effects is apparently dependent upon the lipid:peptide ratio and decreases as the lipid:peptide ratio decreases (data not presented). Thus, the relative proportion of δ-lysin-containing DMPC MLVs and small DMPC particles is a function of the absolute concentration of peptide as well as of the lipid:peptide ratio. The molecular basis of these findings will be discussed later.

We also noted that the thermal history of the sample could affect the thermotropic phase behavior of the DMPC/δ-lysin mixtures, particularly at relatively higher peptide concentrations. Specifically, we compared DSC thermograms of the supernatants of comparable DMPC/δ-lysin mixtures (R = 15:1) after incubation for 1 or 5 h at 55 °C prior to DSC analysis (data not presented). After the longer period of incubation, the DSC endotherm resulting from the DMPC phase transition of the small lipid−peptide particles decreases in temperature, increases in area, and becomes considerably broader. Moreover, the area under the sharp endotherm arising from the large multilamellar vesicles in the pellet decreases. These results indicate that the detergent-like effect of δ-lysin observed at higher peptide concentrations has a kinetic element. In particular, the results suggest that longer periods of incubation result in a relatively greater conversion of large DMPC MLVs to smaller δ-lysin-containing DMPC particles, and that the structure of the particles produced, or the relative amounts of the small unilamellar and discoidal particles present, or both, may be influenced by the period of time in which the peptide and lipid interact, at least above the phospholipid phase transition temperature.

^{31}P NMR Spectroscopic Studies. Figure 4 shows some proton-decoupled ^{31}P NMR spectra of mixtures of DMPC and δ-lysin. The spectra that are shown were acquired at temperatures below (18 °C) and above (35 °C) the temperature range of the main gel to liquid-crystalline phase transition of DMPC in these δ-lysin-containing preparations. At low relative peptide concentrations ($R \cong$ 500:1), the spectra that were obtained exhibit the axially symmetric powder patterns characteristic of fully hydrated phospholipid bilayers. The basal line widths are 90 (18 °C) and 70 ppm (35 °C), values in the range expected for the lamellar gel and liquid-crystalline states of DMPC, respectively. A close inspection of these spectra also shows a small "peak" in the powder pattern occurring near 3.5 ppm downfield, suggesting that there may be a very small population of fast-tumbling phospholipid molecules in the mixture. At a higher relative peptide concentration (R = 62.5:1), the spectra show that the phospholipid population is still predominantly bilayer in arrangement in both the gel and liquid-crystalline states. However, the relative intensity of the sharp peak in the spectrum has increased markedly over that observed at the lower relative peptide concentrations, indicating an increase in the relative proportion of the fast-tumbling DMPC population. At the highest relative peptide concentrations that were examined (R = 30:1), a significant fraction of the population of phospholipids is still in the bilayer conformation in both the gel and liquid-crystalline states, but the spectral intensity from the fast-tumbling population has increased markedly and comprises a significant fraction of the total phospholipids. A close inspection of the "spectral intensities" assigned to the fast-tumbling population of phospholipids (see Figure 5) indicates that, unlike the spectra exhibited at lower relative peptide concentrations, the "sharp" signal can clearly be resolved into two components with peak intensities near 1.9 and 3.5 ppm downfield. The intensity of the downfield component (chemical shift $\cong$ 3.5 ppm) relative to the upfield component is dependent upon the phase state of the bulk lipid phase. In the gel state, the relative intensities of the two components showed little or no change with temperature (T = 4−18 °C); however, there was an abrupt increase in the relative intensity of the downfield peak when the acyl chains melted (T > 28 °C) but no further increases in intensity with increasing temperature. This suggests that at the very high range of relative peptide concentrations that was studied, there are two distinct populations of fast-tumbling phospholipid molecules, as indicated also by the DSC results discussed earlier. The structure of these two

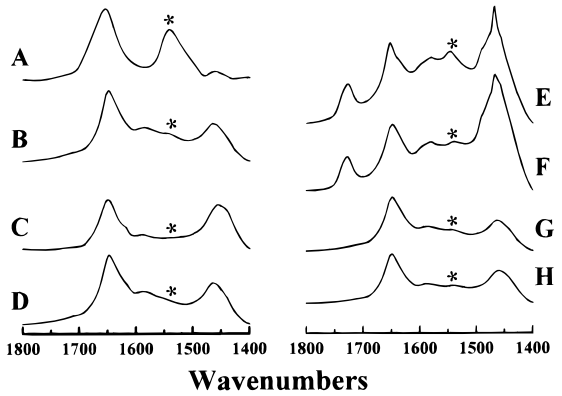

FIGURE 6: Amide I and amide II regions of the infrared spectra of staphylococcal δ-lysin and its mixtures with DMPC. Absorbance spectra are presented for (A) dry lyophilized δ-lysin, (B) a freshly prepared solution in deuterated buffer (0 °C), (C) δ-lysin in deuterated buffer (90 °C), (D) δ-lysin in deuterated buffer (0 °C, recooled from 90 °C), (E) δ-lysin/DMPC (1:15) (freshly prepared dispersion at 10 °C), (F) δ-lysin/DMPC (1:15) (freshly prepared dispersion at 35 °C), (G) δ-lysin in deuterated buffer (freshly prepared solution at 10 °C), and (H) δ-lysin in deuterated buffer (freshly prepared solution at 35 °C). The asterisks mark the positions of the amide II absorption bands centered near 1540 cm^{-1}.

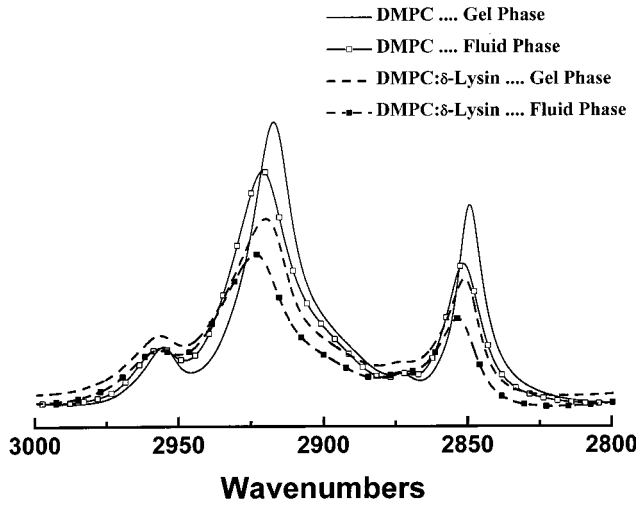

FIGURE 7: C−H stretching region of infrared spectra of DMPC/δ-lysin and DMPC/δ-lysin mixtures (15:1) acquired at temperatures below and above the lipid gel to liquid-crystalline phase transitions. The data were acquired at temperatures near 16 (gel phase) and 34 °C (fluid phase).

populations of small δ-lysin-containing DMPC aggregates will be discussed below.

FTIR Spectroscopic Studies. The left panel in Figure 6 shows the effect of temperature on the amide I and amide II regions of spectra exhibited by a solution of δ-lysin in the D_2O-based buffer used (spectra B−D). The spectrum of the dry lyophilized powder (Figure 6A) is shown as a reference to illustrate the relative sizes of the amide I and amide II bands typically observed in the absence of H−D exchange. In the absence of H−D exchange, the infrared spectrum of δ-lysin exhibits two major absorption bands centered near 1655 and 1540 cm^{-1}. These absorption bands arise from the amide I and amide II vibrational modes of this peptide, respectively (*36*). The observed frequencies of the amide I and II bands are consistent with the peptide being predominantly α-helical under these conditions (*36*). A comparison of spectra A and B of Figure 6 indicates that a large fraction of the amide II absorption band at 1540 cm^{-1} quickly disappears upon dissolution of the peptide in the D_2O-based buffer, and is replaced by a new band centered near 1460 cm^{-1}. This downward shift in band frequency is due to H−D exchange and arises because the amide II vibration contains a sizable contribution from the bending vibrations of the N−H bonds of the peptide backbone (*37*). The fact that a large fraction of the amide II band readily disappears when the peptide dissolves in D_2O indicates that most of the amide I protons of the peptide are easily accessible to the bulk solvent phase and further suggests that the conformation of the peptide is not very rigid. However, there is also a small population of amide protons which exchange fairly slowly with the bulk solvent phase, and under our conditions, complete exchange of this population is only achieved upon heating to temperatures above 70 °C (for an example, see Figure 6C). Most probably, this population of slowly exchanging amide protons arises from amide N−H bonds that are located in the central regions of the peptide helix (for examples of this phenomenon, see refs *38* and *39* and references therein). However, given that δ-lysin is likely to assemble into large aggregates at the peptide concentrations used for these FTIR spectroscopic experiments, it is also possible that the small population of slowly exchanging amide protons arises from peptide bonds which are shielded within the peptide aggregates and are therefore less accessible to the bulk solvent.

Figure 6 also shows that upon dissolution of the peptide in D_2O, the peak frequency of the amide I absorption band shifts downward to frequencies near 1649 cm^{-1}. This observation can also be attributed to amide H−D exchange (*40*), and the amide I frequency observed in D_2O solution is again in the range expected for deuterated α-helical proteins and peptides (*41*). It is also clear that apart from effects that can be attributed to residual H−D exchange, neither the peak frequency nor the shape of the amide I band of δ-lysin changes markedly when solutions of the peptide are heated to temperatures near 90 °C (Figure 6C). Indeed, the only discernible difference between the contours of the amide I band observed at 0 and 90 °C (aside from effects that can be attributed to residual amide H−D exchange) is the appearance of a small shoulder centered near 1620 cm^{-1} at elevated temperatures (Figure 8C). The latter band, which could be attributed to the formation of a small amount of β-like and/or aggregated structures at elevated temperatures (*42, 43*), disappears upon cooling (see Figure 8D), suggesting that the thermally induced structural changes which occur under our conditions are fully reversible. These observations are consistent with the thesis that δ-lysin remains largely α-helical over the temperature range of 0−90 °C under our experimental conditions. Similar conclusions have been drawn from the results of previous FTIR spectroscopic studies of this peptide (*11*).

An examination of spectra E and F of Figure 6 shows that upon interaction of relatively high concentrations of δ-lysin with DMPC (R = 15:1), there is a significant increase in the size of the slowly exchanging population of amide protons (compare spectra E and F with reference solution spectra G and H). This observation suggests that the interaction of δ-lysin with lipid causes a net increase in the population of amide protons that are shielded from the aqueous phase. Such observations have been noted in studies

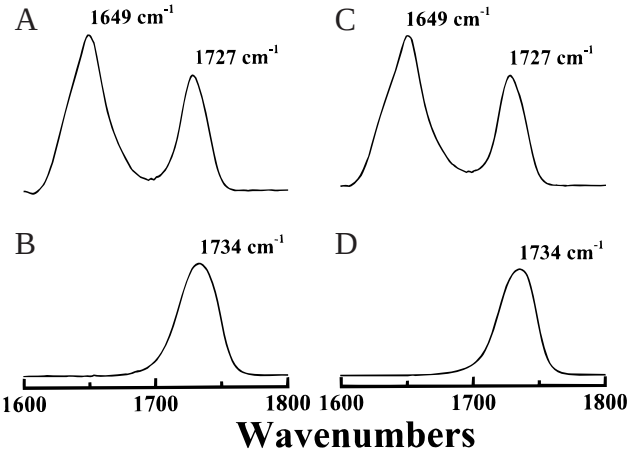

FIGURE 8: Amide I and carbonyl stretching regions of the infrared spectra of staphylococcal δ-lysin and its mixtures with DMPC. The absorbance spectra were recorded in the fluid (left panels) and gel (right panels) phases of aqueous dispersions of DMPC alone (bottom panels) and dispersions of 15:1 DMPC/δ-lysin mixtures (top panels). The data were acquired at temperatures near 10 (gel phase) and 35 °C (fluid phase).

of the interaction of various membrane-associated peptides with lipid micelles or bilayers (*44*−*46*). However, one should also note that a comparison of the relative sizes of the amide II peak in spectrum E with that expected in the absence of H−D exchange (see Figure 6A) indicates that even when associated with DMPC, the slowly exchanging population of amide protons represents only a small fraction of the total population of amide protons that are present. It is also clear that the size of this residual slowly exchanging proton population decreases further when the lipid/peptide mixtures are heated, albeit at rates which are slower than those observed with aqueous solutions of the peptide. We therefore conclude that upon association with DMPC, δ-lysin at high concentrations inhabits an environment that affords some shielding of the peptide from the bulk aqueous phase, but that it is not buried within the hydrophobic domains of the lipid assembly. The probable nature of this environment will be explored more fully below. Unfortunately, it was not possible to carry out similar experiments with much lower peptide concentrations due to the lack of sufficient instrumental sensitivity.

The thermotropic phase behavior of DMPC/δ-lysin mixtures (R = 15:1) was also examined by monitoring the changes occurring in the C−H stretching vibration bands which occur between 2800 and 3000 cm^{-1}. The C−H stretching region of the infrared spectrum of this lipid−peptide aggregate contains two major bands centered near 2850 and 2920 cm^{-1} (Figure 7), which arise from the symmetric and asymmetric methylene stretching vibrations, respectively. With most lipid bilayers, these vibrations give rise to relatively sharp absorption peaks at temperatures below the lipid gel to liquid-crystalline phase transition, and when the lipid hydrocarbon chains melt, the absorption bands broaden and shift upward in frequency by 2−3 cm^{-1}. Such behavior is characteristic of hydrocarbon chain-melting phenomena and results from increases in hydrocarbon conformational disorder and molecular mobility at the chain-melting phase transition (see ref *47* and references therein). As expected, such phenomena were also observed with the samples of pure DMPC and with the DMPC/δ-lysin mixtures used in this study, and these spectroscopic changes were observed over temperature ranges comparable to those of the thermotropic events detected by DSC. This observation is important because it provides evidence that the thermotropic events observed in our DSC experiments, and in particular the sharp and broad components observed in the δ-lysin-rich preparations, all involve the melting of lipid hydrocarbon chains.

To examine the effect of peptide incorporation on the structure and organization of the host lipid bilayer, the infrared absorption bands of the gel and liquid-crystalline phases of pure DMPC were compared with the corresponding bands exhibited by peptide-rich DMPC/δ-lysin mixtures. Our results show that the lipid-specific bands of DMPC alone and of peptide-rich DMPC/δ-lysin mixtures differ significantly in ways which are structurally significant. First, at all the temperatures that were examined, the infrared absorption bands emanating from vibrations of the lipid hydrocarbon chains (e.g., the CH_2 stretching and CH_2 bending bands near 2850 and 1468 cm^{-1}, respectively) tend to be broader in the lipid/peptide mixtures (for example, see Figure 7). This observation suggests that lipid hydrocarbon chains in the peptide-containing DMPC/δ-lysin mixtures are more mobile than those present in peptide-free DMPC vesicles, evidence supporting the existence of structurally different lipid−peptide aggregates at high peptide concentrations (see above). Second, in the CH_2 stretching region of the spectrum, we find that in both the gel and liquid-crystalline states, band maxima of the CH_2 stretching vibrations exhibited by the peptide-rich mixtures occur at slightly higher frequencies than do those of the peptide-free preparations (see Figure 7). Given that increases in the frequencies of these band maxima are generally correlated with increases in lipid hydrocarbon chain conformational disorder (*48*), these results suggest that the incorporation of large quantities of δ-lysin into DMPC bilayers results in an overall increase in hydrocarbon chain disorder in both the gel and liquid-crystalline states. Finally, our data also show that regardless of lipid phase state, the ester C═O stretching band maxima exhibited by the peptide-rich DMPC/δ-lysin mixtures occur at lower frequencies than do those exhibited by the DMPC alone (see Figure 8). With pure DMPC bilayers and with peptide-poor DMPC/δ-lysin mixtures, ester C═O stretching band maxima are generally observed at frequencies near 1733−1735 cm^{-1}, whereas at DMPC:δ-lysin molar ratios near 15:1, these maxima are observed at frequencies near 1726−1728 cm^{-1}. With hydrated phospholipid bilayers, decreases in the frequency of the ester C═O stretching band are generally ascribed to an increase in the population of hydrated or hydrogen-bonded ester carbonyl groups (see ref *47* and references therein). Thus, the lowering of the ester C═O stretching frequency and the increase in the CH_2 stretching and bending frequencies indicate that at high peptide concentrations, δ-lysin induces the formation of structures in which the hydrocarbon chains are highly disordered and the ester C═O groups are located in environments that are more polar and/or more hydrated than in the absence of the peptide. The probable structural basis of these observations is examined in more detail below.

X-ray Diffraction Studies. To obtain additional structural information about the δ-lysin-containing lipid aggregates, an X-ray diffraction analysis was performed. Small-angle X-ray

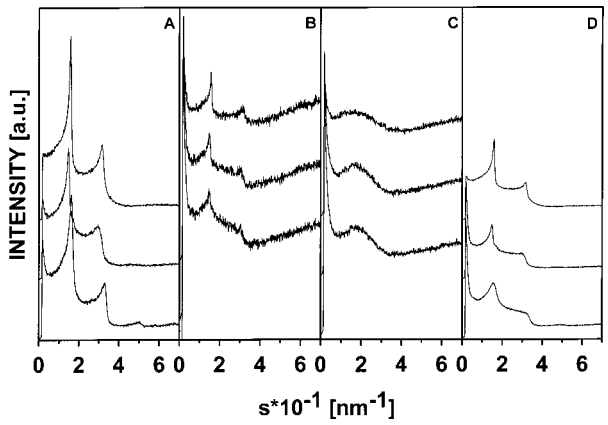

FIGURE 9: Small-angle X-ray diffractograms of pure DMPC (A) and a mixture of DMPC and δ-lysin at a lipid:peptide molar ratio of 62.5:1 (B) as well as of the supernatant (C) and the pellet (D) after centrifugation of the DMPC/δ-lysin sample at 40, 18, and 8 °C (from top to bottom); $s = h/(2\pi)$ and $h = 4(\pi/\lambda)\sin(\Theta)$, where λ is the wavelength of the X-ray beam and 2Θ the scattering angle.

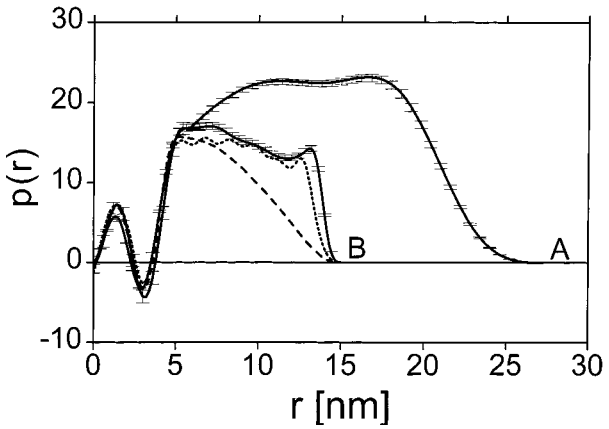

FIGURE 10: Computed pair distance distribution function $p(r)$ of small lipid-containing particles (supernatant) composed of DMPC and δ-lysin at a lipid:peptide molar ratio of 62.5 (A) and 15 (B) derived from experimental scattering data at 18 °C. The experimental errors are represented by error bars. Theoretical $p(r)$ for DMPC/δ-lysin ($R = 15$) at 18 °C obtained from experimental scattering data (solid line) and derived after modeling of a discoidal lipid micelle with a diameter of 14 nm and a bilayer thickness of 5.2 nm (dashed line) as well as of lipid disk (diameter of 12 nm) surrounded by a 1 nm peptide ring (dotted line).

diffractograms obtained from aqueous dispersions of DMPC alone and of a DMPC/δ-lysin mixture ($R = 62.5:1$) are illustrated in Figure 9. The DMPC dispersion (Figure 9A) exhibits scattering profiles with sharp Bragg peaks which are typical for multilamellar vesicles (*49*). The lamellar repeat distances of 6.2 nm ($s = 0.161$ nm^{-1} at 8 °C), 6.8 nm ($s = 0.147$ nm^{-1} at 18 °C), and 6.3 nm ($s = 0.159$ nm^{-1} at 40 °C) are in accordance with earlier and recent X-ray diffraction data from DMPC multilamellar vesicles (*50*, *51*). However, in the presence of the peptide, a significant decrease in the scattering intensities of the Bragg peaks relative to the scattering background, as well as a dramatic increase in the intensity in the innermost part of the scattering curve at an s of <0.05 nm^{-1}, is observed (Figure 9B). These latter features are characteristic of particle scattering and suggest the presence of much smaller lipid−protein aggregates. In fact, the small-angle X-ray diffractograms obtained from the pellet of the lipid/peptide mixture are essentially similar to those obtained with DMPC alone, demonstrating that the pelleted fraction also consists at least primarily of MLVs (Figure 9D), while the scattering curve of the supernatant was characterized by side maxima and minima with a strong maximum around 5.8 nm ($s = 0.17$ nm^{-1}) (Figure 9C). Such features are consistent with the presence of single bilayer particles whose structures will be discussed below. The formation of other structures such as inverted cubic phases, which are also characterized by an isotropic ^{31}P NMR signal, can definitively be excluded by our X-ray scattering measurements, as there was no evidence for additional superimposed Bragg peaks in the X-ray diffractograms.

The intensity of the sharp Bragg peaks typical of MLVs decreases with increasing peptide content. At an R value of 15:1, the first-order Bragg peak was hardly distinguishable from the broad scattering profile (data not shown), which indicates that a large fraction of the DMPC MLVs have been converted into smaller lipid-containing particles at this high peptide concentration.

To obtain additional structural information about the nature of the smaller lipid-containing particles, the experimental X-ray scattering curves of the supernatants with two different peptide contents ($R = 62.5:1$ and 15:1) were subjected to indirect Fourier transformation. The respective computed pair distance distribution functions $p(r)$ for samples in the gel phase are shown in Figure 10. The overall shape of the $p(r)$ function, which reflects the structural properties of the particles in real space, clearly differs between the two lipid:peptide molar ratios and suggests the presence of spherical particles at an R of 62.5:1 (*52*, *53*). The pronounced minimum around an r of 3 nm can be explained by inhomogeneities perpendicular to the bilayer plane of the scattering particle arising from regions with different electron density in the headgroup and the hydrophobic core of the bilayer. These data are thus consistent with the existence of extended lamellar structures such as unilamellar vesicles. For an R of 62.5:1, the calculated $p(r)$ function is characterized by a steep decrease (Figure 10A) when using the largest possible scattering distance D_{max} in the program ITP (*32*), which is constrained by the innermost resolvable h_1 value ($h_1 < \pi_{max}$). This indicates that the real maximum dimension of these peptide−lipid complexes must be larger than 25 nm, where this $p(r)$ function vanishes. Thus, the size of the unilamellar vesicles is beyond the resolution limit of the optical setup used in this experiment. On the other hand, we were able to resolve the maximum dimension for the small lipid-containing particles formed at an R of 15:1, which was estimated to be 15 nm. In addition, the shape of the computed pair distance distribution function of these smaller lipid−peptide aggregates clearly differs from that of the mixture with less peptide in exhibiting a significant local maximum around an r of 13 nm (Figure 10B).

In the case of flat particles such as extended lamellar structures, where the thickness is much smaller than the area, it is possible to derive the one-dimensional distance distribution function [$p(r)$], which provides information about the bilayer structure. Such $p(r)$ functions were calculated for DMPC in the presence of δ-lysin ($R = 15:1$) for the lamellar gel (18 °C) and liquid-crystalline (40 °C) phases. In the fluid phase, a bilayer thickness (d_m) of 4.8 ± 0.2 nm was obtained,

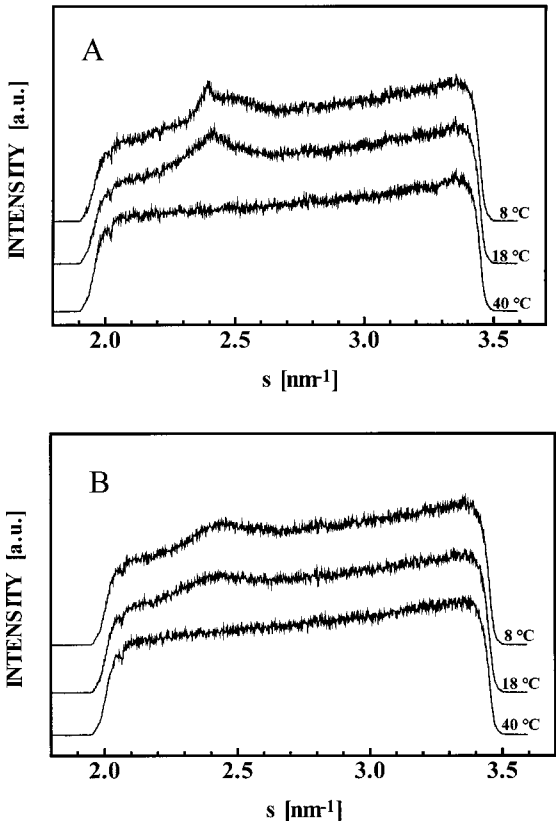

FIGURE 11: Wide-angle X-ray diffractograms of DMPC (A) and a mixture of DMPC and δ-lysin at a lipid:peptide molar ratio of 15:1 (B) at 8, 18, and 40 °C (from top to bottom), where $s = h/(2\pi)$ and $h = 4(\pi/\lambda)\sin(\Theta)$, with λ being the wavelength of the X-ray beam and 2Θ the scattering angle.

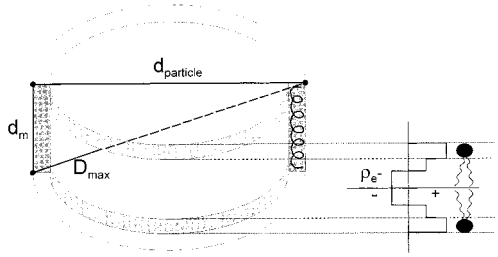

FIGURE 12: Schematic representation of a disk-shaped particle composed of a discoidal lipid bilayer surrounded by a 1 nm peptide ring, with a particle diameter ($d_{particle}$) of 14 nm, a bilayer thickness (d_m) of 5.2 nm, and a maximum particle dimension (D_{max}) of 15 nm. The centrosymmetrically inhomogeneous electron density profile along the bilayer normal is schematically shown with electron densities (relative values on an arbitrary scale) of −15 (inner shell), 10 (middle shell), and 22 (outer shell) and zero being for bulk water.

which is larger than that of pure DMPC, recently reported to be 4.42 nm (*17*). At 8 and 18 °C, d_m was estimated to be 5.2 ± 0.2 nm, which is also significantly larger than that of pure DMPC bilayers (d_m = 4.8 nm at 10 °C) (*54*). This finding can be interpreted by an untilting of the lipid acyl chains owing to a partial penetration of δ-lysin molecules into the hydrophobic core of the lipid bilayer, which is confirmed by our wide-angle X-ray diffraction data. Below the pretransition temperature of pure DMPC, the wide-angle X-ray diffraction pattern (Figure 11A) shows a sharp reflection at 0.418 nm ($s = 2.39$ nm^{-1}) surrounded by a broad band around 0.410 nm ($s = 2.44$ nm^{-1}), which is typical for lipid bilayers in the lamellar gel phase with tilted hydrocarbon chains and pseudohexagonal chain packing (*55*). Above the pretransition temperature, a rather symmetric peak centered around 0.414 nm ($s = 2.41$ nm^{-1}) indicates that the hydrocarbon chains are oriented perpendicular to the bilayer plane and are packed in a hexagonal lattice, as observed for the rippled gel phase. Finally, above the main transition temperature, a diffuse reflection typical for unordered lipid chains in the liquid-crystalline phase was recorded. In the presence of δ-lysin, the sharp peak at 0.418 nm with its shoulder is replaced by a rather symmetric peak around 0.414 nm ($s = 2.42$ nm^{-1}, Figure 11B), indicating that the hydrocarbon chains are oriented perpendicular to the bilayer plane, which is in accordance with an untilting of the acyl chains. Furthermore, in the presence of the peptide, a decrease in the intensity of the maximum peak and a broadening of the diffraction pattern are observed, indicating that the hydrocarbon chain packing becomes less ordered. These observations are consistent with our DSC data, which did not show any pretransition for the supernatants and a strong decrease in the transition enthalpy for the smaller lipid-containing particles, and with our FTIR results, which showed that the infrared absorption bands emanating from vibrations of the lipid hydrocarbon chains (e.g., the CH_2 stretching and CH_2 bending bands near 2850 and 1468 cm^{-1}, respectively) are broader in the lipid/peptide mixtures. The latter observations suggest that the lipid hydrocarbon chains in the peptide-containing DMPC/δ-lysin mixtures are more mobile than those present in peptide-free DMPC vesicles, further supporting the existence of differently packed lipids in peptide-free and peptide-containing lipid aggregates.

Detailed information about the structure of these smaller lipidic aggregates can be obtained by the calculation of theoretical X-ray scattering curves, thereby comparing the simulated and measured pair distance distribution functions. We started our simulations with the simplest model assuming a disk-shaped DMPC bilayer particle. The corresponding theoretical $p(r)$ function is displayed in Figure 10 (dashed line), which is based on the experimentally determined overall particle dimensions, i.e., a d_m of 5.2 nm and a D_{max} of 15 nm, yielding a diameter of 14 nm for the particle. Moreover, the centrosymmetrically inhomogeneous electron density profile along the bilayer normal was approximated by a three-step model for one-half of the bilayer (for the illustration, see also Figure 12). This axial inhomogeneity is due to the fact that the hydrophobic core exhibits low and the hydrophilic headgroup region high relative electron density. Clearly, the $p(r)$ function of such a pure discoidal lipid bilayer does not fit the experimentally obtained $p(r)$ function (Figure 10B). When the molecular properties of DMPC and δ-lysin are considered, a plausible model would be that a peptide ring surrounds a lipid disk, as shown schematically in Figure 12. This model requires the disaggregation of multimeric δ-lysin molecules into dimers or monomers upon interaction with DMPC, which may be promoted by the chaotropic properties of the choline headgroup (*56*). Furthermore, δ-lysin was shown to have a high degree of flexibility along its long axis (*56*), whose length can vary between 3.15 and 4.85 nm. This would be sufficient to span the hydrophobic region of the bilayer, since the

phosphorus−phosphorus distance between phospholipid headgroups in opposite monolayers (see Figure 12), estimated from the maximum of the $p(r)$ function, is 3.4 nm in the liquid-crystalline phase and 4.0 nm in the gel phase. These considerations suggest that the hydrophobic face of the amphipathic helix interacts with the hydrophobic edge of the DMPC disk, thereby preventing its energetically unfavorable exposure to the aqueous environment. However, our experimental approach and analysis does not allow us to determine the actual orientation of the peptide helix in the disk-shaped micelle. There may also be some peptide within the bilayer and not just at the rim of the disk, as suggested by the presence of some peptide in the MLVs. Moreover, the phospholipid may partially curve around the edges of the disk where it interacts with the peptide. However, the general features of our model are supported by the results of our FTIR measurements, which indicate that at high concentrations, δ-lysin exists in an environment that affords some shielding of the peptide from the bulk aqueous phase but that the peptide is not buried within the hydrophobic domains of the lipid assembly.

To model the monomolecular peptide ring surrounding the lipid disk, we used a thickness of 1 nm, which was reported to be the cross-sectional area of the δ-lysin helix (*56*). To simulate the rim of the peptide layer around the disk, we successively increased the relative electron density (ρ) of this peptide ring from zero corresponding to water to a value corresponding to the relative electron density of the headgroup region, which we had taken in our model (see also Figure 12). These simulations showed that increasing the relative electron density of the peptide rim caused an increase of the weighting of the large distances around an r of 13 nm, which is reflected in the local maximum of the $p(r)$ function. This is in contrast to a smooth decay toward zero for the particle distance distribution function for a model corresponding to a pure DMPC discoidal particle. The same characteristics were found for the experimental $p(r)$ function (Figure 10B), and thus, we can conclude that the local maximum of the $p(r)$ function around 13 nm reflects the electron-dense region of the peptide rim surrounding the DMPC bilayer disks. The best fit between the experimental and theoretical $p(r)$ function (Figure 10B, dotted line) was obtained for a ratio of relative electron density of the phospholipid headgroup region to peptide of 0.82. This ratio is in a reasonable agreement with a value of 0.74 which can be calculated from the experimental absolute electron density values reported for PC headgroups (0.45 electron/Å^3) (*57*) and the calculated electron density values for proteins (0.42 electron/Å^3) and for water (0.34 electron/Å^3). Moreover, taking into account the cross-sectional area of DMPC molecules in a gel phase lipid bilayer (0.46 nm^2) (*58*) as well as that of the δ-lysin helix (1 nm) (*56*), one can calculate a lipid:peptide molar ratio of about 12:1, which is in good agreement with the experimental value gained from our lipid and peptide analysis of the supernatant.

DISCUSSION

Perhaps the major new finding arising from this work is that DMPC/δ-lysin mixtures containing higher concentrations of peptide consist of two macroscopically distinct populations of aggregates. One population of aggregates consists primarily of large multilamellar vesicles containing relatively smaller amounts of peptide, whereas the higher-density aggregates consist of much smaller lipid-peptide particles containing relatively larger amounts of peptide. Calorimetrically, the thermotropic phase behavior of DMPC in each of these two lipid−peptide complexes is somewhat different. In the δ-lysin-containing DMPC multilamellar vesicles, the incorporation of increasing quantities of peptide has almost no effect on the temperature of the pretransition or of the main transition, although the cooperativity of both of these transitions is reduced modestly and their transition enthalpies are reduced considerably, particularly at low peptide concentrations. In contrast, in the small δ-lysin-containing lipid/peptide particles, a pretransition is completely absent and the temperature of the main phase transition is increased somewhat, the cooperativity is reduced markedly, and the phase transition enthalpy is greatly reduced. Moreover, at the highest peptide concentration that was tested, two overlapping broad, higher-temperature endotherms are resolved by calorimetry in the population of small aggregates. These differences in calorimetric behavior are also correlated with differences in spectroscopic behavior. Specifically, the ^{31}P NMR spectra of the δ-lysin-containing large multilamellar vesicles are those characteristic of the lamellar gel or liquid-crystalline phases of DMPC when present in a relatively large vesicle tumbling slowly on the NMR time scale. In contrast, the isotropic ^{31}P NMR spectra of the smaller δ-lysin/DMPC particles are characteristic of DMPC molecules undergoing motional averaging on the ^{31}P NMR time scale. Such isotropic NMR spectra could arise from DMPC molecules in a lamellar state but undergoing rapid isotropic tumbling, or from DMPC molecules present in nonlamellar (normal micellar or reversed cubic) phases (*59*). The X-ray diffraction data presented here support the first alternative, and suggest that δ-lysin-containing small unilamellar vesicles and discoidal particles are both present. Moreover, the DSC and ^{31}P NMR spectroscopic methods are in good quantitative agreement as well, in that only the large δ-lysin-containing multilamellar vesicles are observed by both techniques at lower peptide concentrations (DMPC:peptide molar ratios of $\geq$125:1), whereas progressively increasing populations of the δ-lysin-containing small DMPC/peptide particles are present as peptide concentrations increase to DMPC:peptide molar ratios of $\leq$62.5:1. As well, at the two higher δ-lysin concentrations that were tested (DMPC:peptide molar ratios of 30:1 and 15:1), two-component broad endotherms are detected by DSC and two isotropic signals are detected by ^{31}P NMR spectroscopy, indicating the presence of two types of small lipid/peptide particles, as well as smaller quantities of δ-lysin-containing DMPC large multilamellar vesicles.

Our calorimetric findings are in broad agreement with the earlier DSC and TSD results published by Lohner et al. (*23*), which covered a lower range of peptide concentrations (minimum DMPC:peptide molar ratio that was investigated was 30:1). In that study, the pretransition was reported to decrease in enthalpy with little change in temperature or cooperativity, as we find here. However, Lohner et al. (*23*) reported that the pretransition was abolished at the highest peptide concentration that was tested, whereas the results presented here, on both the intact samples and the centrifugally resolved multilamellar vesicles and small peptide/lipid particles, clearly reveal the persistence of the pretransition

in the vesicular fraction, even at a DMPC:peptide molar ratio of 15:1. Moreover, the observation by Lohner et al. (*23*) of the presence of a broader endotherm at higher temperatures only at the highest peptide concentration that was tested (30:1) also agrees with the results presented here. The failure of Lohner et al. (*23*) to detect the pretransition at a DPPC:*δ*-lysin molar ratio of 30:1 is probably due to a lower DSC instrumental sensitivity, although differences in the PC that was utilized and also possibly differences in the absolute lipid and peptide concentrations that were used in these two studies may explain this discrepancy (see below).

Our ^{31}P NMR results are also generally comparable to those reported earlier by Dufourc et al. (*24*) and Rydal and Macdonald (*25*). However, the former authors both reported that an isotropic ^{31}P NMR signal only appeared in DPPC/*δ*-lysin or POPC/*δ*-lysin mixtures, respectively, at molar ratios of $<$10:1, whereas only lamellar phase signals were present at all lower peptide concentrations. In contrast, although our results are qualitatively similar to theirs, we detect the presence of an isotropic ^{31}P NMR signal at much lower peptide concentrations (DMPC:*δ*-lysin molar ratios of $\leq$62.5:1). Moreover, similar quantitative results are seen in this study by DSC and by X-ray diffraction. We thus ascribe these differences in the quantitative but not qualitative results of these three studies primarily to our use of a different phospholipid, since Bhakoo et al. (*22*) has reported that *δ*-lysin appears to interact more strongly with shorter-chain than with longer-chain phospholipid bilayers. However, as before, differences in the absolute peptide and lipid concentrations utilized in these studies, and in the thermal history of the samples, may also have made some contribution to these quantitative variations in results.

The comparative effects of the incorporation of *δ*-lysin on the thermotropic phase behavior of zwitterionic and anionic phospholipid bilayers can also be used to deduce both the general location of this peptide relative to the lipid bilayer and the nature of the lipid−peptide interactions that are involved. For example, Papahadjopoulos et al. (*60*) and McElhaney (*26*) have proposed that many membrane-associated proteins can be classified into one of three groups with regard to their interactions with phospholipid bilayers. Group I proteins are typically positively charged, water soluble, peripheral membrane proteins that interact much more strongly with anionic than with zwitterionic lipids. The interactions of such proteins with anionic phospholipid bilayers typically increase both the temperature and enthalpy of the main phase transition temperature while decreasing its cooperativity only slightly. Group I proteins are localized on the bilayer surface where they interact only with the phospholipid polar headgroups primarily by electrostatic interactions. Group II proteins are also typically positively charged at neutral pH but are somewhat less water soluble and also interact more strongly with anionic than with zwitterionic phospholipid bilayers. The interactions of these proteins with anionic phospholipid bilayers usually decrease the temperature, enthalpy, and cooperativity of the main phase transition moderately, at least at relatively high protein concentrations. Group II proteins are localized at the bilayer interface where they interact primarily with the polar headgroups and glycerol backbone region of the phospholipid molecules by both electrostatic and hydrogen bonding interactions, although some hydrophobic interactions with the region of the hydrocarbon chains near the bilayer interface also occur. Finally, group III proteins have a range of charges but are typically water insoluble, integral membrane proteins that interact equally well with anionic and zwitterionic phospholipid bilayers. The effect of the incorporation of such proteins into phospholipid bilayers is usually to alter the temperature only slightly but to decrease the enthalpy and cooperativity of the main phase transition markedly. Group III proteins penetrate into or through phospholipid bilayers and interact with the phospholipid hydrocarbon chains by hydrophobic and van der Waals interactions, as well as with the phospholipid polar headgroups. The incorporation of group I proteins also usually has little effect on the permeability of the anionic phospholipid vesicles with which they interact, while the incorporation of group II and group III proteins increases vesicle permeability. The results of this study indicate that in large multilamellar vesicles, *δ*-lysin behaves initially most like a group III protein, since its incorporation has no effect on the temperature of the DMPC chain-melting phase transition, but decreases the cooperativity and especially the enthalpy markedly. Moreover, the effects of *δ*-lysin on the thermotropic phase behavior of DMPG and DMPC are very similar, indicating little anionic phospholipid specificity for this peptide (unpublished observations). The marked decrease in enthalpy in particular indicates that *δ*-lysin must substantially perturb DMPC hydrocarbon chain packing in the gel state and/or increase the extent of DMPC hydrocarbon chain packing in the liquid-crystalline state, suggesting that this peptide penetrates deeply into or through the hydrophobic core of the bilayer. Indeed, the TSD results of Lohner et al. (*23*), which indicate that *δ*-lysin substantially reduces the volume change at the main phase transition of DPPC vesicles, support this view. However, this interpretation does not seem to be compatible with the ^{2}H NMR studies of *δ*-lysin-containing DPPC vesicles by Dufourc et al. (*24*), who reported that *δ*-lysin had no effect on hydrocarbon chain orientational order in the gel state. This latter finding is surprising, since almost all naturally occurring amphipathic or hydrophobic peptides or proteins studied to date disorder phospholipid hydrocarbon chains in the gel state (see refs *61* and *62*).

At relatively high peptide concentrations, *δ*-lysin produces small DMPC−peptide aggregates with a slightly elevated phase transition temperature and a markedly reduced cooperativity and transition enthalpy. The progressive conversion of large multilamellar DMPC vesicles to smaller particles likely explains the second marked decline in overall enthalpy observed at higher peptide concentrations in this study (Figure 2). The reduced cooperativity and enthalpy of the smaller aggregates are relatively easy to rationalize, since small unilamellar phospholipid vesicles produced, for example, by sonication, have substantially reduced cooperativity and enthalpy compared to the multilamellar vesicles from which they are derived (see ref *26*). Similarly, the small DMPC/*δ*-lysin discoidal particles also produced at higher peptide concentrations would be expected to undergo a hydrocarbon chain-melting transition with reduced cooperativity and enthalpy, because of these relatively small numbers of phospholipid molecules in each particle and the perturbation of hydrocarbon chain packing by the presence of the peptide molecules in contact with the lipid hydrocarbon

chains at the edges of the disk. In fact, the FTIR studies presented here confirm this prediction. However, in both cases one might also have predicted that the gel state of these smaller DMPC/δ-lysin mixtures might also have been disordered by the peptide, resulting in a decrease, rather than a small increase, in the phase transition temperature. Apparently, however, the δ-lysin molecules are able to stabilize these structures in some manner which is not clearly apparent to us at present. Alternatively, the presence of δ-lysin molecules could also in principle destabilize the liquid-crystalline phase to a greater extent than the gel phase, possibly by an increased extent of penetration of peptide into fluid bilayers. Additional experimental work will be required to address this issue further.

Our DSC and ^{31}P NMR results on DMPC/δ-lysin mixtures, at a constant molar ratio but varying absolute concentrations of lipid and peptide, also indicate that the concentration-dependent state of aggregation of this peptide probably has an effect on its interaction with the host lipid bilayer. In particular, at higher absolute peptide concentrations, δ-lysin appears to perturb DMPC hydrocarbon chain packing to a greater degree on a per mole basis than at lower absolute concentrations, as manifested by a reduced enthalpy of the DMPC hydrocarbon chain-melting phase transition. Additional studies of this phenomenon will be required to elucidate its molecular basis.

These FTIR findings of a predominantly α-helical δ-lysin conformation in both aqueous buffer and small unilamellar vesicles or discoidal particles are for the most part similar to these other studies of the conformation of this peptide reviewed in the introductory section. In addition, our studies indicate that the helical conformation of this peptide is quite stable even at higher temperatures. Given the small size of this molecule, such observations may be attributable to the formation of multimolecular aggregates at the peptide concentrations that were used (*13*). Moreover, our results are closely similar to those reported by Brauner et al. (*11*) for δ-lysin interacting with DPPC- and POPC-oriented bilayers, where a predominant amide I peak with a frequency centered at 1657 cm^{-1} dominated their spectra, with very minor contributions from components located at 1635 and 1680 cm^{-1}, indicating a mostly α-helical conformation with small amounts of β-antiparallel pleated sheet structure in this particular model membrane system. The decrease in the hydrocarbon orientational order and the increase in the motional freedom of these oriented lipid membranes in the presence of peptide reported by these workers are also in accord with the effects of δ-lysin on DMPC hydrocarbon chain organization in the small peptide−lipid aggregates studied here. It thus appears that δ-lysin retains its overall predominantly α-helical conformation in lipid micelles, monolayers, bilayers, or discoidal particles, although its state of aggregation is probably not identical in each of these systems. It would have been of interest to investigate whether the considerable degree of D−H amide exchange noted with the small discoidal particles produced by high δ-lysin concentrations studied here would also be observed at much lower peptide concentrations, where only multilamellar vesicles are formed, but unfortunately, technical limitations precluded these experiments because the amide I and II absorption were too low in such systems to produce adequate spectra for such an analysis.

Our X-ray diffraction studies have shown that at high peptide concentrations, the action of δ-lysin on DMPC multilamellar vesicles leads to the formation of disk-shaped lipid−peptide aggregates probably consisting of a disk-shaped lipid bilayer surrounded by an annulus of δ-lysin molecules. Similar effects of the amphipathic α-helical bee venom toxin, melittin, which also consists of 26 amino acids, on multilamellar PC vesicles have been reported (*63*, *64*). Most interestingly, disk-shaped particles were also found for DMPC/melittin mixtures (molar ratio of 15:1) at 10 °C. A hydrodynamic radius of 6.9 nm, i.e., a diameter of 13.8 nm, was estimated for the DMPC/melittin particles by gel filtration (*63*), in excellent agreement with the results from our small-angle X-ray scattering data, which yield a particle size of 14 nm for DMPC/δ-lysin particles at 8 and 18 °C.

The formation of discoidal lipid particles was recently identified for other amphipathic α-helical peptides, e.g., for glucagon, a 29-amino acid polypeptide hormone (*65*). The formation of such disks is not unique to amphipathic peptides, but has also been reported from much larger proteins, namely, apoproteins. Apolipophorin III, a hemolymph protein of the Sphinx moth (*66*), and the important plasma protein apolipoprotein E or domains thereof (*67*), are able to form disks upon interaction with DMPC. For the former, uniform disk-like structures with an average diameter and width of 18.5 and 4.8 nm, respectively, were reported (*68*). In the latter, the orientation of the helices was suggested as a ring around the disks whereby the helices are parallel to the bilayer plane. Such an arrangement was also suggested for melittin ("bicycle-tire" model), as a result of its proline kink, which causes a bend angle of about 120°, resulting in its "banana-like" shape (*69*).

Discoidal structures can also be observed in reconstituted high-density lipoprotein particles (*70*). They contain little or no core lipid and are distinct from typical detergent micelles in that they cannot exist in the absence of apolipoproteins (*71*). Like other phospholipid-binding proteins, apoA1 is made up of a series of amphipathic helical segments, typically 22 amino acids long. This is again an interesting structural analogy to the overall conformation and length of staphylococcal δ-lysin. Like our model, these helices form a ring around the disk, whereby the helices were determined to be aligned parallel to the lipid chains (*72*). The thickness of these particles is 3.5 nm, which corresponds again to the length of the 22 amino acid helices. Although differences exist, it is interesting to find such similar structures upon the interaction of peptides or proteins with simple lipid systems which in living cells fulfill different biological functions.

REFERENCES

1. Freer, J. H., and Arbuthnott, J. P. (1983) *Pharmacol. Ther. 19*, 55−106.
2. Thelestam, M. (1983) in *Staphylococci and Staphylococcal Diseases* (Easman, C. S. F., and Easman, C. A., Eds.) Vol. 2, pp 705−744, Academic Press, London.
3. Bernheimer, A. W., and Rudy, B. (1986) *Biochim. Biophys. Acta 864*, 123−141.
4. Kreger, A. S., Kim, K. S., Zaboretsky, F., and Bernheimer, A. W. (1971) *Infect. Immun. 3*, 449−465.
5. Kapral, F. A. (1972) *Proc. Soc. Exp. Biol. Med. 141*, 519−521.

6. Fitton, J. E., Dell, A., and Shaw, W. V. (1980) *FEBS Lett. 115*, 209−212.
7. Colacicco, G., Basu, M. I., Bucklew, A. R., and Bernheimer, A. W. (1977) *Biochim. Biophys. Acta 465*, 378−390.
8. Fitton, J. E. (1981) *FEBS Lett. 130*, 257−260.
9. Tappin, M. J., Pastore, A., Norton, R. S., Freer, J. H., and Campbell, I. D. (1988) *Biochemistry 27*, 1643−1647.
10. Lee, K. H., Fitton, J. E., and Wuthrich, K. (1987) *Biochim. Biophys. Acta 911*, 144−153.
11. Brauner, J. W., Mendelsohn, R., and Prendergast, F. G. (1987) *Biochemistry 26*, 8151−8158.
12. Alouf, J. E., Dufourcq, J., Siffert, O., Thiaudiere, E., and Geoffrey, C. (1989) *Eur. J. Biochem. 183*, 381−390.
13. Thiaudiere, E., Siffert, O., Talbot, J. C., Bolard, J., Alouf, J. E., and Dufourcq, J. (1991) *Eur. J. Biochem. 195*, 203−213.
14. Garone, L., Fitton, J. E., and Steiner, R. F. (1988) *Biophys. Chem. 31*, 231−245.
15. Freer, J. H., and Birkbeck, T. H. (1982) *J. Theor. Biol. 94*, 535−540.
16. Lohner, K., and Epand, R. M. (1997) *Adv. Biophys. Chem. 467*, 1−11.
17. Kantor, H. S., Temple, B., and Shaw, W. V. (1972) *Arch. Biochem. Biophys. 151*, 142−156.
18. Birkbeck, T. H., and Whitelaw, A. D. (1980) *J. Med. Microbiol. 13*, 213−218.
19. Yianni, Y. P., Fitton, J. E., and Morgan, C. G. (1986) *Biochim. Biophys. Acta 856*, 91−100.
20. Morgan, C. G., Fitton, J. E., and Yanni, Y. P. (1986) *Biochim. Biophys. Acta 863*, 129−138.
21. Bhakoo, M., Birkbeck, T. H., and Freer, J. H. (1982) *Biochemistry 21*, 6879−6883.
22. Bhakoo, M., Birkbeck, T. H., and Freer, J. H. (1985) *Can. J. Biochem. Cell Biol. 63*, 1−6.
23. Lohner, K., Laggner, P., and Freer, J. H. (1986) *J. Solution Chem. 15*, 189−198.
24. Dufourc, E. J., Dufourcq, J., Birkbeck, T. H., and Freer, J. H. (1990) *Eur. J. Biochem. 187*, 581−587.
25. Rydall, J. R., and Macdonald, P. M. (1992) *Biochim. Biophys. Acta 1111*, 211−220.
26. McElhaney, R. N. (1986) *Biochim. Biophys. Acta 864*, 361−421.
27. Lewis, R. N. A. H., Mak, N., and McElhaney, R. N. (1987) *Biochemistry 26*, 6118−6126.
28. Lewis, R. N. A. H., and McElhaney, R. N. (1985) *Biochemistry 24*, 2431−2439.
29. Mantsch, H. H., Madec, C., Lewis, R. N. A. H., and McElhaney, R. N. (1985) *Biochemistry 24*, 2440−2446.
30. Laggner, P., and Mio, H. (1992) *Nucl. Instrum. Methods Phys. Res., Sect. A 323*, 86−90.
31. Glatter, O. (1980) *J. Appl. Crystallogr. 13*, 577−584.
32. Glatter, O. (1977) *J. Appl. Crystallogr. 10*, 415−421.
33. Glatter, O. (1982) in *Small-Angle X-ray Scattering* (Glatter, O., and Kratky, O., Eds.) pp 119−166, Academic Press, London.
34. Glatter, O. (1982) in *Small-Angle X-ray Scattering* (Glatter, O., and Kratky, O., Eds.) pp 167−196, Academic Press, London.
35. Mittelbach, P., and Porod, G. (1961) *Acta Phys. Austriaca 14*, 405−439.
36. Miyazawa, T., and Blout, E. R. (1960) *J. Am. Chem. Soc. 82*, 712−719.
37. Miyazama, T., Shimaouchi, T., and Mizushima, S. (1958) *J. Chem. Phys. 29*, 611−616.
38. Zhang, Y.-P., Lewis, R. N. A. H., Henry, G. D., Sykes, B. D., Hodges, R. S., and McElhaney, R. N. (1995) *Biochemistry 34*, 2348−2361.
39. Nakanishi, M., Tsuobi, M., Ikegami, A., and Kamehisa, M. (1972) *J. Mol. Biol. 64*, 363−378.
40. Chigadze, Y. M., and Brazhnikov, E. V. (1974) *Biopolymers 13*, 1701−1712.
41. Dwivedi, A. M., and Krimm, S. (1984) *Biopolymers 23*, 923−943.
42. Middaugh, C. R., Mach, H., Ryan, J. A., Sanyah, G., and Velkin, D. B. (1995) *Methods Mol. Biol. 40*, 137−156.
43. Pribic, R., van Stokkum, I. H. M., Chapman, D., Harvis, P. I., and Blumenthal, M. (1993) *Anal. Biochem. 214*, 366−378.
44. Sami, M., and Dempsey, C. (1988) *FEBS Lett. 240*, 211−215.
45. Englander, J. F., Downer, N. W., and Englander, S. W. (1987) *J. Biol. Chem. 275*, 7982−7986.
46. Henry, G. D., Weiner, J. H., and Sykes, B. D. (1987) *Biochemistry 26*, 3626−3634.
47. Lewis, R. N. A. H., and McElhaney, R. N. (1996) in *Infrared Spectroscopy of Biomolecules* (Mantsch, H. H., and Chapman, D., Eds.) pp 159−202, John Wiley & Sons, New York.
48. Maroncelli, M., Strauss, H. L., and Snyder, R. G. (1985) *J. Chem. Phys. 82*, 2811−2824.
49. Laggner, P. (1994) in *Subcellular Biochemistry: Physicochemical Methods in the Study of Biomembranes* (Hilderson, H. J., and Ralston, G. B., Eds.) Vol. 23, pp 451−492, Plenum Press, New York.
50. Janiak, M. J., Small, D. M., and Shipley, G. G. (1976) *Biochemistry 15*, 4575−4580.
51. Petrache, H. I., Tristam-Nagle, S., and Nagle, J. F. (1998) *Chem. Phys. Lipids 95*, 83−94.
52. Müller, K. (1981) *Biochemistry 20*, 404−414.
53. Glatter, O. (1991) *Prog. Colloid Polym. Sci. 84*, 46−54.
54. Laggner, P. (1982) in *Small-Angle X-ray Scattering* (Glatter, O., and Kratky, O., Eds.) pp 329−359, Academic Press, London.
55. Tardieu, A., Luzatti, V., and Reman, F. C. (1973) *J. Mol. Biol. 75*, 711−733.
56. Thiaudière, E., Siffert, O., Talbot, J.-C., Bolard, J., Alouf, J. E., and Dufourcq, J. (1991) *Eur. J. Biochem. 195*, 203−213.
57. Wiener, M. C., Suter, R. M., and Nagle, J. F. (1989) *Biophys. J. 55*, 315−325.
58. Seddon, J. M. (1993) in *Phospholipid Handboo*k (Cevc, G., Ed.) pp 936−937, Marcel Dekker, New York.
59. Gruner, S. M., Cullis, P. R., Hope, M. J., and Tilcock, C. P. S. (1985) *Annu. Rev. Biophys. Biophys. Chem. 14*, 211−238.
60. Papahadjopoulos, D., Moscarello, M., Eylar, E. H., and Issac, T. (1975) *Biochim. Biophys. Acta 401*, 317−335.
61. Bloom, M., and Smith, I. C. P. (1985) in *Progress in Lipid−Protein Interactions* (Watts, A., and De Pont, J. J. H. H. M., Eds.) Vol. 1, pp 143−172, Elsevier, Amsterdam.
62. Marsh, D. (1985) in *Progress in Lipid-Protein Interactions* (Watts, A., and De Pont, J. J. H. H. M., Eds.) Vol. 1, pp 143−172, Elsevier, Amsterdam.
63. Dufourcq, E. J., Faucon, J.-F., Fourche, G., Dasseux, J.-L., Maire, M. L., and Gulik-Krzywicki, T. (1986) *Biochim. Biophys. Acta 859*, 33−48.
64. Faucon, J.-F., Donmatin, J.-M., Dufourcq, J., and Dufourcq, E. J. (1995) *Biochim. Biophys. Acta 1234* (2), 235−243.
65. Ryu, K.-S., Han, H.-S., and Kim, H. (1998) *J. Biochem. 123*, 55−61.
66. Raussens, V., Narayanaswami, V., Goormagtigh, E., Ryan, R. O., and Ruysschaert, J.-M. (1998) *J. Biol. Chem. 271*, 23089−23095.
67. Raussens, V., Fisher, C. A., Goormagtigh, E., Ryan, R. O., and Ruysschaert, J.-M. (1998) *J. Biol. Chem. 272*, 25825−25830.
68. Wientzek, M., Kay, C. M., Oikawa, K., and Ryan, R. O. (1994) *J. Biol. Chem. 269*, 4605−4612.
69. Dempsey, C. E. (1990) *Biochim. Biophys. Acta 1031*, 143−161.
70. Jonas, A. (1992) in *Structure and Function of Apolipoprotens* (Rosseneu, M., Ed.) pp 218−250, CRC Press, Boca Raton, FL.
71. Fielding, P. E., and Fielding, C. J. (1996) in *Biochemistry of Lipids, Pipoproteins and Membranes* (Vance, D. E., and Vance, J., Eds.) pp 495−516, Elsevier, Amsterdam.
72. Fielding, P. E., and Fielding, C. J. (1995) *J. Lipid Res. 36*, 211−228.

BI9913101